An NMR study of the geometry of a CO layer chemisorbed on Pt particles

J. Ph. Ansermet, C. P. Slichter, and J. H. Sinfelt

Citation: The Journal of Chemical Physics **88**, 5963 (1988); doi: 10.1063/1.454509
View online: http://dx.doi.org/10.1063/1.454509
View Table of Contents: http://scitation.aip.org/content/aip/journal/jcp/88/9?ver=pdfcov
Published by the AIP Publishing

An NMR study of the geometry of a CO layer chemisorbed on Pt particles

J. Ph. Ansermet and C. P. Slichter
Department of Physics and Materials Research Laboratory, University of Illinois, Urbana, Illinois 61801
J. H. Sinfelt
Exxon Research and Engineering Company, Annandale, New Jersey 08801

(Received 7 October 1987; accepted 29 January 1988)

The authors have analyzed the shape of the ^{13}C spin echo envelope of a ^{13}CO layer chemisorbed on supported Pt particles. They show that it contains information about the geometry of the array of molecules on the surface. They find that two mechanisms are responsible for the shape. The coupling of the C spins with the surface Pt spins gives rise to a T_2 of 2.9 ms at 77 K. By applying a Carr–Purcell sequence to the ^{13}C spins, the effects of the coupling to the Pt can be eliminated. The dipolar coupling between ^{13}C molecules then remains, producing a "slow beat" in the spin echo envelope. It can be analyzed exactly since mutual spins flips among C spins are not allowed, owing to large field inhomogeneities at the surface of the Pt particles. Analysis of the slow beat yields information about the structure of the array. The authors report evidence for the coalescence of islands of CO at low coverage and demonstrate that the coverage is uneven among the Pt particles if the sample powder is exposed to less than a monolayer of CO.

I. INTRODUCTION

We report the use of NMR to study the geometry of an array of atoms or molecules chemisorbed on supported metal particles. The classic method to study such problems is by techniques such as low energy electron diffraction (LEED), applied to oriented single crystal surfaces. There is a vast literature reporting beautiful and intricate results. Such methods are not applied to supported metal particles. Therefore, in studying such particles it is useful to have other means to check the state of the sample to see, for example, whether the single crystal results apply to the small metal particles. In particular, when using NMR to study aspects of such samples it is useful to be able to characterize the spacing between adjacent molecules. While the NMR cannot give the complete pattern of an array of molecules, as we show, it can test among potential patterns, or tell whether the molecules are close together or far apart, an important consideration when the surface coverage is partial.

Analysis of the dipolar broadening of NMR line shapes is commonly used to study the structure of crystals and molecules. In the case of molecules adsorbed on metal particles, the situation is complicated by the paramagnetic susceptibility of the metal and by chemical shift anisotropies. At the applied field necessary to detect signals with a reasonable amount of averaging, these two effects broaden the line enormously.

On the other hand, spin echoes can be used to refocus field inhomogeneities while leaving the spin–spin coupling intact. Therefore the decay of the spin echo as a function of the time between the 90° and the 180° pulses can be used to study the intermolecular dipolar coupling, so long as other relaxation mechanisms do not dominate the relaxation.

We have used the spin echo technique to measure at 82 kG the transverse relaxation of ^{13}C spins in a layer of ^{13}CO chemisorbed on supported Pt particles. We have found that the dipolar coupling among the ^{13}C spins plays a major role in the decay of the spin echo amplitude as the time between the 90° and 180° pulses is increased. In most cases in NMR, only the first few moments of a line can be calculated. But here it is possible to calculate the complete dipolar line shape exactly because the field inhomogeneity is very large compared to the dipolar coupling. We will explicitly derive the Fourier transform of the line shape, which is the time dependence of the echo decay.

In earlier works, Wang in our group used measurements of the transverse relaxation of ^{13}C–^{13}C pairs to determine the C–C bond lengths of chemisorbed molecules.[1] In this article, we show how we can make use of transverse relaxation measurements to get information on the geometry of a layer of chemisorbed CO.

II. SAMPLES

The samples are made of Pt particles, 10 to 50 Å in diameter, supported on an alumina substrate. More information about our samples can be found elsewhere.[2,3] CO gas is chemisorbed at room temperature and the samples are sealed in glass vials. Unless it is explicitly mentioned, we used CO gas enriched to 90% of ^{13}CO. Since the sealed samples are kept on shelves for a long time, the CO molecules can diffuse on the surface of the particles and reach an equilibrium. On the other hand, all NMR data are taken at temperatures so low (most often at 77 K) that diffusion rates are extremely slow on the time scale of NMR experiments.

We label our samples by indicating successively: the metal, the dispersion, the chemisorbed gas, and the coverage if it is not saturation coverage (e.g., Pt-41–CO-7.5%). The dispersion is the percentage of metal atoms at the surface. It is measured by hydrogen chemisorption. The coverage is determined by exposing the cleaned samples to just enough molecules to produce that coverage. An exception to this procedure is the production of saturation coverage samples. In that case, the cleaned samples are exposed to more gas molecules than the metal surface can chemisorb, and after a while the physisorbed CO is pumped out.

 0021-9606/88/095963-09$02.10

III. THE MECHANISMS CAUSING THE DECAY OF THE ECHO ENVELOPE

A. A first look at the data

Figure 1 shows some essential results. It displays the echo height vs the evolution time, which is the time interval between the 90° pulse and the echo. We shall refer to such curves as echo envelopes. The crosses show the decay of the echo envelope in a sample at saturation coverage where CO is highly enriched in ^{13}C. The envelope decays monotonically over a time interval of the order of 1 ms. These data were taken with excellent signal-to-noise ratio and they do not fit either a simple exponential or a Gaussian relaxation. This decay is due primarily to the C–C dipolar coupling, as we will show in the following experiment and as we describe theoretically in Sec. IV.

In order to estimate the importance of relaxation mechanisms which do not involve the ^{13}C–^{13}C dipolar coupling, we have prepared a sample where the ^{13}CO gas was diluted in ^{12}CO. As we will see in Sec. IV, a 9% ^{13}CO dilution insures that the distance between ^{13}CO molecules is so large that the dipolar coupling is negligible. The triangles in Fig. 1 show that the decay of the echo envelope of the isotopically diluted sample is a single exponential with $T_2 = 2.3$ ms. Hence the decay is much slower than it is in a sample highly enriched in ^{13}CO. We conclude that the ^{13}C–^{13}C dipolar coupling plays a major role in the relaxation of our 90% ^{13}C enriched CO.

B. Effect of the surface Pt spins

What causes the decay of the spin echo envelope in a sample where the ^{13}CO molecules are diluted in ^{12}CO molecules?

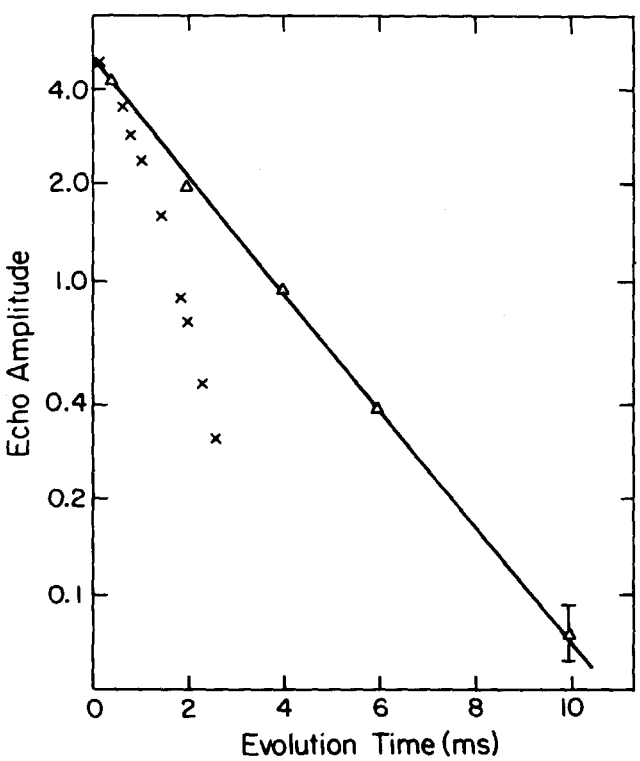

FIG. 1. Echo envelope vs evolution time for samples at saturation coverage; (×) Pt-76–CO, 90% ^{13}CO, (Δ) Pt-48–CO, 10% ^{13}CO.

We will show evidence that the decay arises from the fluctuations of the ^{195}Pt spins of Pt atoms attached to CO molecules. As will appear in Sec. IV, knowledge of the origin of this relaxation mechanism is not necessary in order to deduce geometrical information from the spin echo data, so long as the value of the T_2 corresponding to this coupling is known. Nonetheless, we present our analysis because we find that such a coupling to the metal surface can be of fundamental importance in NMR studies of adsorbed molecules.

The coupling between the ^{13}C spins of chemisorbed CO and the ^{195}Pt spins of surface Pt atoms was measured in a double resonance experiment performed earlier in our group.[4] Makowka *et al.* found that the direct ^{195}Pt–^{13}C coupling and the indirect spin–spin coupling through the Pt–CO bond induce local fields at the ^{13}C nucleus, H_L, of the order of 1.3 G. We define the quantity a as

$$a = \gamma(H_L) \tag{1}$$

to represent the Pt–C coupling in units of angular frequency. γ is the ^{13}C gyromagnetic ratio. The spin echo sequence used in the present paper is a single resonance experiment. It refocuses the line broadening produced by the Pt spins so long as the Pt spins do not flip during the experiment. If they do flip, then the echo height is reduced. The Pt spin flips can be caused by Pt T_1 processes or by Pt–Pt mutual spin flips. We call τ the mean time between Pt spin flips.

If there were no other line broadening mechanisms, and if τ were infinite, the coupling of the ^{195}Pt spins to the ^{13}C nucleus would split the ^{13}C resonance into two lines, one for each orientation of the ^{195}Pt spin, separated in angular frequency by a. If, however, the Pt spin is undergoing spin flips, the situation is modified. This problem was analyzed using the Bloch equations by Hahn[5] and Slichter.[6] (See also Appendix F of Ref. 7.) There are two limiting regimes distinguished by how the mean times between Pt flips τ compares with $1/a$, the reciprocal of the splitting frequency.

In what is commonly referred to as the weak collision limit:

$$a\tau \ll 1, \tag{2}$$

the relaxation time for the C spins is

$$1/T_2 = a^2\tau. \tag{3}$$

Likewise, in the strong collision limit,

$$a\tau \gg 1, \tag{4}$$

the C spins get completely dephased between two Pt flips, and $T_2 = \tau$.

We can tell that we are in the strong collision limit by comparing T_2 with the known coupling a. Figure 2 shows $1/T_2$ between 4 and 300 K for the sample of ^{13}CO diluted in ^{12}CO. At 77 K, for example, the T_2 is about 2.3 ms. If we were in the weak collision limit we would have τ of the order of 15 μs from Eq. (3). In the strong collision regime, we would have a τ of 2 ms.

15 μs is much too short compared to the Pt T_1 or the Pt mutual spin flip rate. We have measured the ^{195}Pt T_1 at 77 K in the sample where ^{13}CO is diluted in ^{12}CO [i.e., Pt-48–CO (9% ^{13}CO)]. We found a T_1 of 3.8 ± 0.5 ms. We cannot

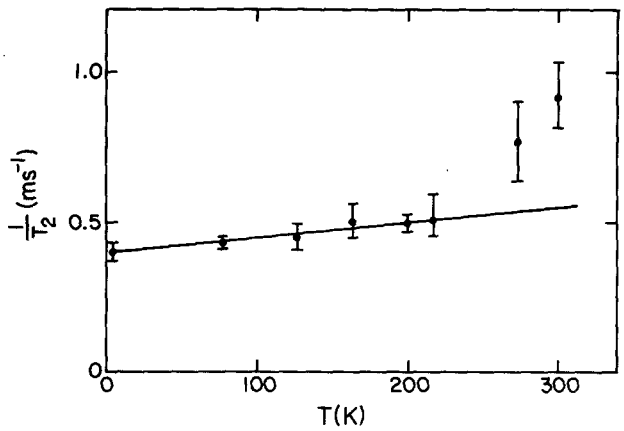

FIG. 2. Temperature dependence of the ^{13}C T_2 of Pt-48–CO (9% ^{13}CO).

measure the Pt mutual spin flip rate because the Pt T_2 is dominated by slow beat effects.[8] However we can set an upper limit on the rate with which Pt neighbors can undergo mutual spin flips by assuming the neighbors have the same resonant frequency. The Pt J coupling in the metal is very strong (about 4 kHz). A spin will then exchange orientation with a neighbor in a time τ of $1/(2J)$, or 125 μs. This is much too slow to account for the 15 μs τ. It can, however, probably account for a τ of 2 ms in a higher order process in the presence of the large field inhomogeneities produced by the paramagnetic susceptibility of the Pt particles.

Hence the value of τ deduced in the strong collision limit is of the right order of magnitude compared to the Pt T_1 and some mutual spin flips partially hindered by the field inhomogeneities at the surface of the particles. The exact relationship between the rate of Pt spin flips and the ^{13}C T_2 is difficult to establish theoretically because the next nearest Pt neighbor to a CO molecule does contribute somewhat to the relaxation of the ^{13}C spins and because only 33.7% of the Pt nuclei have a nuclear moment.

Figure 2 shows that above 250 K the ^{13}C T_2 rapidly gets much shorter. We attribute this effect to the diffusion of CO, a completely different phenomenon which we discussed elsewhere.[9]

The ^{195}Pt spin flips relax the ^{13}C spins too quickly to permit us to observe the true ^{13}C dipolar slow beat when the ^{13}C's are present in low abundance. Therefore, it would be desirable to find some experimental method effectively to turn off the ^{195}Pt–^{13}C coupling. We turn now to such a method.

In order to see what to do, it is useful to reflect on how the relaxation goes in the strong collision case. As we have noted, if there were no other broadening mechanism, and if the ^{195}Pt spins were not flipping, the ^{195}Pt–^{13}C coupling would split the ^{13}C resonance into two lines. If a ^{195}Pt neighbor were in a particular spin state, such as spin up, the ^{13}C would precess at the frequency of one of these lines. Since ^{195}Pt nuclei are found with essentially equal probability with spin up or spin down, one half the ^{13}C spins would precess at each frequency. This would cause the two groups to get out of phase with each other but the 180° pulse of the ^{13}C spin echo sequence refocuses them so that they get back in phase at the time of the echo. If, however, a Pt spin should flip, the ^{13}C nucleus to which it couples would suddenly change its precessional angular frequency by a or $-a$. It will then get out of phase with the other spins in a time of order $1/a$. Since $a\tau \gg 1$, we see that the spin gets out of phase completely long before the next time its neighboring ^{195}Pt has a spin flip. (The fact that a single jump causes a rapid loss of phase coherence is the basis for the term "strong collision" limit.) It is this loss of phase coherence we wish to prevent.

The trick is to apply a damage limiting approach—we apply pulses to the ^{13}C nuclei which prevent a loss of phase coherence. This is done by use of a Carr–Purcell pulse sequence[7] which consists of an initial 90° pulse, followed at a time $\tau_{cp}/2$ by a sequence of π pulses spaced apart in time by τ_{cp}. Then, if there are no ^{195}Pt spin flips, the ^{13}C spins never deviate in phase by more than $\pm (a\tau_{cp}/4)$ from the precession phase they would have with $a = 0$ (i.e., no ^{195}Pt–^{13}C coupling). Suppose now a ^{195}Pt flips during one cycle. A detailed look shows that this can at most produce a phase error of $\pm a\tau_{cp}/2$. Since the jump can occur at any time, the mean square phase error turns out to be $\frac{4}{3}(a\tau_{cp}/4)^2$.

Since the phase errors are of either sign, depending on where in the cycle the jump occurs, N such jumps will produce a mean square phase error $\overline{\Delta^2\phi}$ given by

$$\overline{\Delta^2\phi} = N\tfrac{4}{3}\left(\frac{a\tau_{cp}}{4}\right)^2. \tag{5}$$

If the mean time between jumps is τ, one will accumulate 1 rad of root mean square deviation in a time T given by

$$1 = \frac{T}{\tau}\frac{4}{3}\left(\frac{a\tau_{cp}}{4}\right)^2 \tag{6}$$

or

$$\frac{1}{T} = \frac{1}{\tau}\frac{4}{3}\left(\frac{a\tau_{cp}}{4}\right)^2. \tag{7}$$

We take T to be the decay time of the ^{13}C magnetization resulting from ^{195}Pt spin slips. Clearly we can make T as long as we please by making τ_{cp} sufficiently short.

The condition for the onset of the desired effect is

$$a\tau_{cp}/4 \leqslant 1. \tag{8}$$

Notice that the Carr–Purcell sequence enables us to convert the loss of ^{13}C phase coherence from the strong collision case in which one Pt flip leads to complete phase loss, to the weak collision case for which it now takes many flips of a ^{195}Pt neighbor to dephase the ^{13}C.

From Fig. 3 we see that when $\tau_{cp} = 1$ ms, T is about twice its value τ without the Carr–Purcell sequence. That enables us to conclude that

$$a \cong 0.4 \times 10^3 \text{Hz} = 2.5 \times 10^3 \text{ rad/s}. \tag{9}$$

Makowka *et al.* found by ^{195}Pt–^{13}C double resonance that the direct coupling of a ^{195}Pt to a ^{13}C was about 1.3 kHz. Since only 33% of the Pt are ^{195}Pt, many of the COs are not bonded directly to a ^{195}Pt. It is thus reasonable to get a somewhat less than the Makowka value.

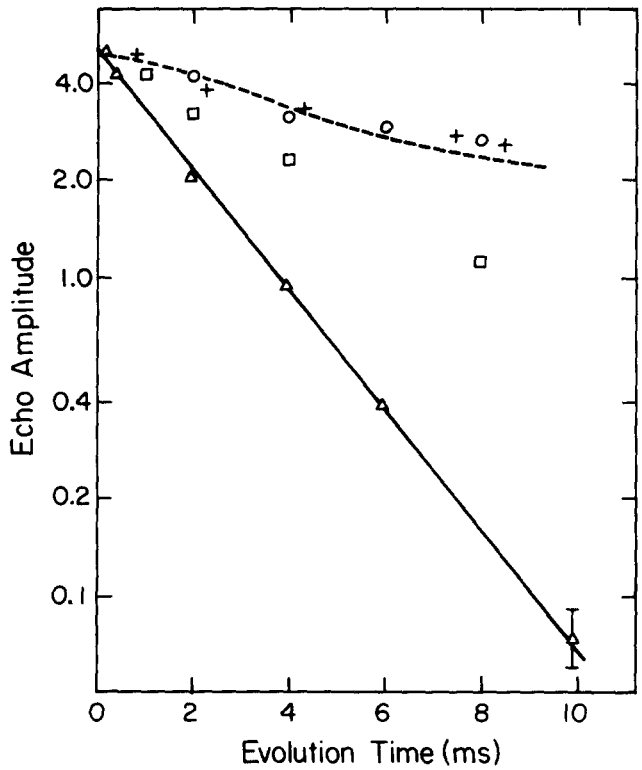

FIG. 3. Pt-48–CO (9% ^{13}CO), echo envelope without (△) and with a Carr–Purcell train of π pulses separated by an interval of 1 ms (□), 250 μs (○), 130 μs (+). Dashed line: effect residual dipolar coupling (see the text).

The residual decay is consistent with the weak C–C dipolar coupling of ^{13}CO molecules far away from each other. The dashed line in Fig. 3 is the result of a calculation (explained in Sec. IV) of the dipolar coupling among CO molecules for a so called $c(4\times2)$ CO pattern on a Pt(111) face with 9% of the sites occupied by ^{13}CO.

If we take into account the effect of the residual C–C dipolar coupling measured by the Carr–Purcell experiment in the limit of closely spaced 180° pulses, we find that the actual T_2 due to the coupling to Pt spins is 2.9 ms. We will assume that the value of T_2 is the same for all molecules, whether they are bridge bonded or linear bonded, on a Pt(100) face or a Pt(111). If the T_2 were quite different for different sites, we would see several components to the decay of the echo envelope of the diluted sample.

C. Ruling out relaxation by ^{13}C–^{13}C mutual spin flips

We show now that a relaxation through ^{13}C mutual spin flips is not possible. The magnitude of the magnetic field, H_{CC}, arising at one ^{13}C due to a neighboring ^{13}C separated by a distance r is

$$H_{CC} = \frac{\gamma\hbar}{r^3}[3\cos^2(\theta) - 1]/2, \qquad (10)$$

where $\hbar$ is Plank's constant and γ is the gyromagnetic ratio of ^{13}C. θ is the angle between the C–C axis and the applied field. As we will see in Sec.IV A, the shortest distance r which we had to consider in fitting the spin echo envelope data was 3.65 Å. Therefore H_{CC} is at most 0.2 G. Two spins can undergo a mutual spin flip only if the difference in precession frequencies is smaller than the dipolar coupling. We were able to demonstrate experimentally that mutual spin flips are not allowed by showing that no cross relaxation could take place within a time of the order of the spin–lattice relaxation time.[9] The simple argument which follows shows that the field inhomogeneity at the surface of the Pt particles is in fact much larger than the dipolar coupling, thus making mutual spin flips impossible.

There are two factors which contribute to the field inhomogeneity at the surface of the Pt particles. One is the ^{13}C chemical shift of CO, the other is the demagnetizing field produced by the Pt particles. On a given face of a Pt particle, all CO molecules have the same orientation with respect to the magnetic field. If the neighboring molecules are of a different kind (e.g., bridge and linear), NMR data on Pt carbonyl clusters[10] tells us that one can expect differences in the isotropic values of the chemical shift of more than 50 ppm (4 G in 80 kG). Hence the field differences in this case are clearly larger than the dipolar coupling.

If the molecules are bonded at similar sites (e.g., all bridge, or all linear) the chemical shift anisotropy does not contribute to the field differences between adjacent adsorption sites. On the other hand, unlike the chemical shift anisotropy, the Pt demagnetizing field varies across a given face. In order to estimate its magnitude, we will approximate the shape of the Pt particles by a sphere.

Assuming that the particles are spherical, the Pt demagnetizing field at the surface is

$$H_{Pt} = \frac{8\pi\chi H_0}{3}[3\cos^2(\theta) - 1]/2, \qquad (11)$$

where χ is the Pt susceptibility (20.6×10^{-6} in CGS volume units).[11] The applied field H_0 is 82 kG for all experiments, hence H_{Pt} varies over a range of about 21 G. Naturally, it is possible for two CO molecules to be positioned in such a way that the difference in H_{Pt} at the two positions is much smaller than H_{CC}. When two CO molecules are positioned at the same θ, the field difference vanishes. But the field gradients at the surface of the particles are so large that only a small fraction of the ^{13}C molecules are in such a configuration. One can easily calculate the probability for a CO molecule to have a neighbor 3.65 Å away in a direction with respect to the applied field such that the field difference is less than the coupling H_{CC}. This probability is less than 3% for particles of 20 Å in diameter, which corresponds to the largest particle size in the samples used for this study.[2] Our NMR data are not sensitive to a slight modification in the behavior of less than 10% of the total magnetization.

D. Slow beat for an array of spins

When the difference in precession frequencies of neighboring spins is large compared to the dipolar coupling between them, mutual spin flips are not allowed, and the dipolar coupling does not contribute to the transverse relaxation. Nonetheless a decay of the spin echo envelope may arise from the dephasing produced by the dipolar fields of neighboring spins. This effect is called the slow beat phe-

nomenon. A description of this effect using an operator formalism is given in the Appendix.

A more intuitive description of the slow beat can be derived from a consideration of the dephasing in the precession of each spin caused by the dipolar field produced by the neighboring spins. The Hamiltonian of the dipolar coupling between two "unlike" spins can be written as

$$H_{d0} = \hbar A\,[1 - 3\cos^2(\theta)]I_{1z}I_{2z}, \tag{12}$$

where

$$A = \gamma^2\hbar/r^3. \tag{13}$$

After a time t the dephasing produced by the dipolar field of a nearby nucleus is (ωt) where

$$\omega = \pm A\,[3\cos^2(\theta) - 1]/2. \tag{14}$$

If each spin has N neighbors producing a dephasing $(\omega_i t)$ by the ith neighbor then the echo amplitude after a time t is

$$B(t) = \cos\left(\sum_{i=1}^{N}\omega_i t\right). \tag{15}$$

Given a certain configuration of sites on the surface, we can calculate the average of $B(t)$ over all the possible values of ω. We will consider the case where not all the sites are occupied. The fact that an unoccupied site would not produce any dephasing can be represented by artificially adding 0 as a possible value for I_z. If f is the fraction of sites which are occupied, then $I_z = \pm 1/2$ with a probability $f/2$ and $I_z = 0$ with a probability $1-f$. Then[12]

$$\begin{aligned}\langle\cos(\Sigma\omega_i t)\rangle &= \mathrm{Re}[\exp(it\Sigma\omega_i)] \\ &= \mathrm{Re}\prod_{i=1}^{N}\langle\exp(it\omega_i)\rangle \\ &= \mathrm{Re}\prod_{i=1}^{N}(f/2\exp(it|\omega_i|) \\ &\quad + f/2\exp(-it|\omega_i|) + 1 - f) \\ &= \prod_{i=1}^{N}[f\cos(\omega_i t) + 1 - f]. \end{aligned} \tag{16}$$

Finally we have to calculate a powder average corresponding to all the possible orientations of the surface with respect to the applied field. This calculation can easily be done numerically. Therefore, once we assume a certain pattern for the CO layer on the surface, we can calculate $B(t)$ with no adjustable parameters.

IV. ANALYSIS OF THE SLOW BEAT FOR VARIOUS CO COVERAGES

The results of Sec. III can be summarized by expressing the decay of the echo envelope as

$$M(t) = M_0 B(t)\exp(-t/T_2), \tag{17}$$

where $B(t)$ represents the slow beat phenomenon and T_2 characterizes the relaxation due to the coupling to the surface Pt spins.

The exponential term was deduced from the T_2 measurement for the diluted sample (Fig. 1). After a small correction for the residual slow beat effect (see Fig. 3 and Sec. III B) we found a T_2 of about 2.9 ms.

In order to calculate the slow beat $B(t)$, we need to make some assumptions about the relative distances between CO molecules. We chose to use the CO patterns observed on Pt single crystal surfaces by low energy electron diffraction (LEED) measurements. This allows us to compare adsorption on single-crystal surfaces to that on small particles.

The shape of supported Pt particles is commonly thought to approximate cubooctahedra. If this is indeed the case, then the surface of the particles consists of large Pt(111) faces and small Pt(100) faces and we can calculate the slow beats of CO patterns for these crystalline faces.[13]

The actual shape of the particles is still debated. While some electron microscopy studies confirm the idea that the particles exhibit mostly (111) faces,[14] others give evidence for particles having mostly (100) faces.[15] Our particles are smaller than the typical particles of these studies, we do not really know what the shape of our particles is.

We cannot use our slow beat analysis to tell whether the particles exhibit mostly (111) or (100) faces. There is more than one combination particle shapes and CO patterns which can produce the same slow beat $B(t)$. Complications in the interpretation may arise from surface reconstruction or contraction of the CO layer itself.

Nonetheless since the dipolar coupling is inversely proportional to the cube of the internuclear distance, the slow beat is very sensitive to the density of CO molecules. The essential results of our data analysis do not rely heavily on any assumption about the shape of the particles.

We make the simple assumption that the particles are cubooctahedra in order to express the density of the CO layers in a very pictorial way. We can then explore the sensitivity of the analysis to the presence of different CO patterns on Pt faces.

We have found no significant difference in the echo envelope of a sample of very large particles (dispersion of 15%) and a sample of very small particles (dispersion of 76%). This is not surprising. Since the doplar coupling is inversely proportional to the cube of the distance between spins, only the near neighbors of each spin contribute a significant amount to the slow beat. Consequently we have calculated the slow beats for various patterns assuming that the particle faces were infinite.

A. CO layer at high coverage

At high coverage, most of the molecules are on (111) faces since cubooctahedra have predominantly (111) faces. Two CO patterns have been seen on Pt(111) faces: a so-called $c(4\times2)$ pattern at high coverage and a $(\sqrt{3}\times\sqrt{3})R\,30°$ pattern at low coverage.[17] The meaning of these terms can be seen from Fig. 4. Assuming that at high coverage CO is adsorbed on Pt particles with the same $c(4\times2)$ pattern observed on Pt(111) faces, we get an excellent fit to the data (Fig. 5, curve A). On the contrary, assuming a $(\sqrt{3}\times\sqrt{3})R\,30$ pattern does not fit the data at all (Fig. 5, curve B). The nearest-neighbor distance from a $c(4\times2)$ pattern is 3.65 Å. It is 4.80 Å in a $(\sqrt{3}\times\sqrt{3})R\,30$ pattern. Hence, we see how sensitive the slow beat is to the distance between nearest-neighbor molecules.

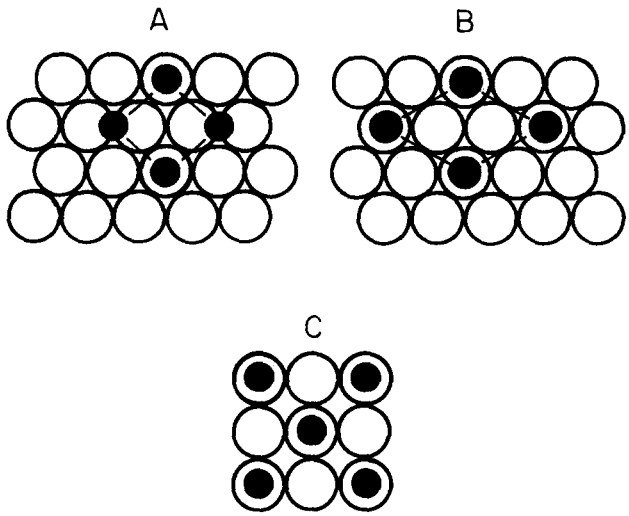

FIG. 4. (A) $c(4\times2)$ pattern on a (111) face; (B) $(\sqrt{3}\times\sqrt{3})R\,30°$ on a (111) face; (C) $c(2\times2)$ on a (100) face.

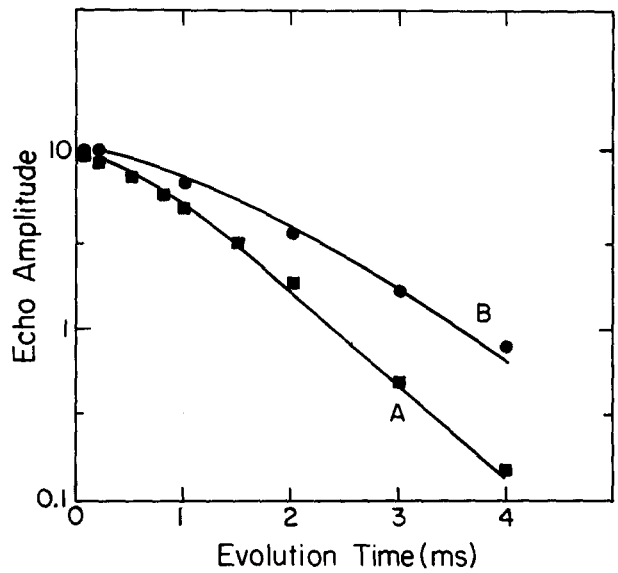

FIG. 6. Echo envelope at 77 K of Pt-41–CO (33%): (■) before, (●) annealing. Curve A: 20% $c(4\times2)$ 100% occupied and 80% $c(2\times2)$ 100% occupied. Curve B: 33% $c(2\times2)$ 100% occupied and 67% $(\sqrt{3}\times\sqrt{3})R\,30°$ with occupancy of 0.23/0.33.

We are not thereby demonstrating that the surface of the particles consists mostly of (111) faces. An excellent fit of the data can also be obtained if we assume a $c(2\times2)$ pattern on a Pt(100) with a slight contraction of all CO distances by a factor 1.08. This contraction could for example account for a coverage of 58% instead of 50%.

B. CO layer at intermediate coverage

It is well known that when a supported metal catalyst is exposed to a very small amount of gas, the metal particles are not evenly exposed to the gas. The gas molecules chemisorb on the most accessible metal particles and consequently never reach metal particles in the interior of the sample. NMR evidence for this phenomenon has been previously reported by de Menorval and Fraissard.[18] Our analysis of the slow beat of CO allows us to observe this phenomenon in our samples.

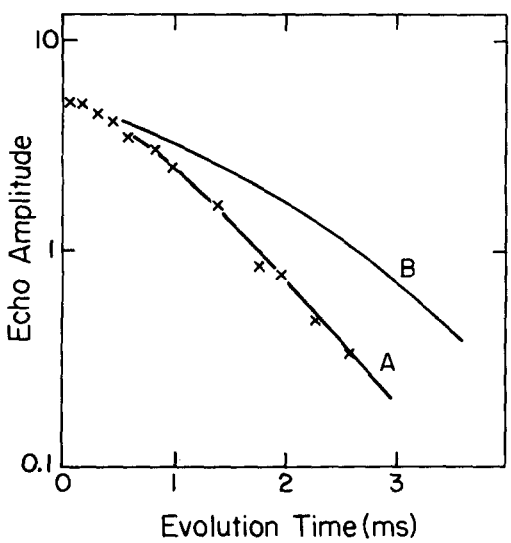

FIG. 5. Pt-76–CO echo envelope at 77 K. Solid curves are theoretical calculations of: (A) slow beat of $c(4\times2)$ pattern on Pt(111) slow beat of $(\sqrt{3}\times\sqrt{3})R\,30°$ on Pt(111). The Pt effects are in the calculation, with $T_2 = 2.9$ ms.

We have prepared a sample with a coverage of 33% (Pt-41–CO-33%). Figure 6 shows that, upon chemisorption at room temperature, the decay of the echo envelope appears almost identical to that of a full coverage sample. In fact, the data fit a combination of 20% of a slow beat of $c(2\times2)$ on (100) faces and 80% of a slow beat of $c(4\times2)$ on (111) faces, both patterns being fully occupied. [Spin-lattice relaxation data[9] confirm that we need to consider the CO molecules on the (100) faces.]

We then annealed the sample for two days at 550 K, far above the desorption temperature,[19] in order to guarantee that the CO molecules could migrate throughout the sample. After this annealing, the echo envelope changed drastically, as can be seen in Fig. 6. We can explain this change if the molecules had initially adsorbed to give high coverage on a few particles only and if the anneal allowed the molecules to rearrange to lower coverage among all the particles of the sample.

The slow beat of the annealed sample is consistent with the assumption that the (100) faces are fully covered, while the (111) faces are partially covered and the molecules on the (111) faces are randomly distributed. Justification for assuming that the (100) faces are fully covered will appear in the next section. Note that if the molecules formed islands on the (111) faces, the decay would be analogous to that of a fully covered sample, and consequently much faster (curve A of Fig. 6)!

The echo envelope of the annealed sample also fits the slow beat corresponding to a random distribution of the CO molecules over the entire particle surface. In that case, one would have 20% of $c(2\times2)$ with an occupancy of 0.32/0.50, and 80% of $(\sqrt{3}\times\sqrt{3})R\,30°$ occupied to 100%.

This simply means that a sample with a coverage of 33% cannot be used to prove clumping on (100) faces. We show in the next section that a coverage of about 10% provides the best test for island formation.

C. CO layer at low coverage

Where do the molecules adsorb at low coverage? Do they adsorb at edges and corners? Are they scattered throughout the surface, or do they clump together? The clumping of CO molecules has been observed on single crystal surfaces and is referred to as island formation. After a controversial debate in the literature of UHV studies, it was concluded that island formation on Pt(100) faces resulted from a removal of the Pt surface reconstruction which is induced by the CO chemisorption and which increases the binding energy of CO.[20]

We have prepared a low coverage sample (Pt-41–CO-7.5%) to try to answer these questions. We maintained our sample at about 500 K for a day in order to allow the CO molecules to desorb many times and distribute themselves evenly in the catalyst powder. We have evidence from spin–lattice relaxation data that the sample does not consist of a few Pt particles having a high CO coverage.[9] This sample exhibits a single T_1 while for all samples at high CO coverage, a broad distribution of T_1 is seen.

Figure 7 shows that the echo envelope data for the low coverage sample are not very different from the data at high coverage. Since the slow beat phenomenon plays a major role in the spin echo decay, we can readily say that the relative distances between molecules are not very different at high or at low coverage. (The scatter in the data is higher for the low coverage sample than for the high coverage sample simply because the signal is much weaker and the signal-to-noise ratio is low even after extensive signal averaging.)

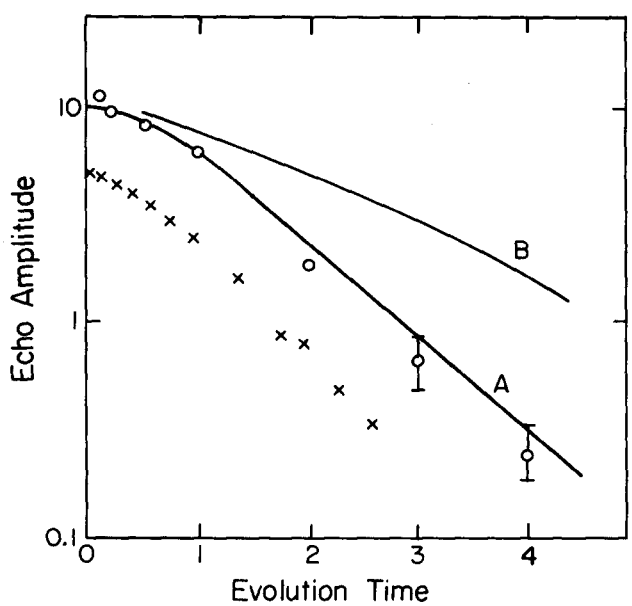

FIG. 7. Echo envelope at 77 K: (O) Pt-41–CO-7.5%; (x) Pt-76–CO. Solid curves are theoretical calculations of (A) slow beat of $c(2\times2)$ pattern on a (100) face; (B) slow beat of $(\sqrt{3}\times\sqrt{3})R$ 30° pattern on a (111) face, with 15% of the sites occupied.

We now consider several possible arrangements of the CO molecules which do not fit the data, and then some which do. At coverages less than 30%, CO on Pt(111) forms a $(\sqrt{3}\times\sqrt{3})R$ 30° pattern.[17] If the molecules were randomly distributed on the Pt particles, the slow beat would be approximately that of $(\sqrt{3}\times\sqrt{3})R$ 30° pattern with only 15% of the sites occupied. This is not the case, or the decay would be a lot slower than for the high coverage sample [Fig. 7(b)]. On the other hand, if at low coverage the molecules were absorbed at corners and edges, the slow beat would be very much like that of a linear chain. If the CO molecules were alternatively linearly bonded and bridged bonded, they would be 4.15 Å apart. If they were all linearly bonded, they would be 2.77 Å apart. We tried many other cases. All of them yield a relaxation which is too slow.

Several possible arrangements of the molecules at the surface of the particles give rise to slow beats which fit the data. For example, the observed decay at low coverage can be accounted for if one assumes that the CO molecules form a $c(4\times2)$ pattern on (111) faces which is 70% occupied. Since we have no evidence for island formation on (111) faces from our study of the sample at intermediate coverage, this is not a reasonable assumption.

It is possible to find fully occupied patterns which fit the data. For example, a $c(2\times2)$ pattern has been observed on (100) faces at high coverage.[21] It has a slow beat which indeed fits the data reasonably well (Fig. 7). The fact that CO would cluster on small facets of the Pt catalyst is not surprising. Thermal desorption spectroscopy indicates that large differences in adsorption energies are to be expected.[19] A mere difference in adsorption energies of $\Delta E = 1.5$ kcal/mol yields a Boltzmann factor

$$\exp\left(-\frac{E}{kT}\right)$$

of less than 10% at 300 K.

V. CONCLUSION

We have analyzed the echo envelopes of a layer of ^{13}CO molecules chemisorbed on Pt particles. We have been able to identify two relaxation mechanisms.

We have singled out a relaxation mechanism which is independent of the C–C dipolar coupling by preparing a sample where the ^{13}CO molecules were diluted with ^{12}CO. We have shown that this relaxation arises from coupling of the ^{13}C to the surface ^{195}Pt spins and have shown that we can eliminate this source of relaxation by use of a Carr–Purcell pulse sequence.

Mutual spin flips associated with the ^{13}C–^{13}C dipolar coupling are ruled out owing to the large field inhomogeneity at the surface of the Pt particles.

The slow beat phenomenon is very sensitive to the nearest-neighbor distance between CO molecules. Consequently we have been able to infer geometric properties of a layer of chemisorbed CO from measurements of transverse relaxation. In particular, the transverse relaxation at low and at high CO coverages is identical within experimental error, hence indicating that, at low coverage, the CO molecules formed islands on the Pt particles. Such islands could simply

correspond to the fact that the CO molecules first adsorb on some small faces of the particles.

We have also noted that the echo envelope at intermediate coverage decayed in much shorter time before than after annealing at 550 K, above the CO desorption temperature. Therefore, when a cleaned sample is exposed to less CO molecules than necessary to get full coverage, the CO molecules reach only a fraction of the Pt particles.

ACKNOWLEDGMENTS

We thank our collaborators Po-Kang Wang, Zhiyue Wang, and Serge L. Rudaz for numerous discussions. This work was supported in part by the Department of Energy, Division of Materials Research, Contract No. DE-ACO2-76ER01198. We gratefully acknowledge the receipt of a Fellowship (J.Ph. A.) from the Exxon Education Foundation.

APPENDIX

We use the operator formalism[22–24] to calculate the slow beat of N spins 1/2. The Hamiltonian is

$$H = H_{d0} + H_z + H_{rf}, \tag{A1}$$

where

$$\begin{aligned} H_{d0} &= \hbar\sum_{i\neq j} a_{ij} I_{iz} I_{jz}, \\ H_z &= \hbar\sum_i \gamma \Delta h_i I_{iz}, \\ H_{rf} &= \hbar\sum_i \gamma H_1 I_{ix}. \end{aligned} \tag{A2}$$

For convenience, we omit the proportionality constants in the expression for the density matrix $\rho(0)$ at thermal equilibrium. Thus we simply write

$$\rho(0) = \sum_i I_{iz}. \tag{A3}$$

If $\tau/2$ is the time interval between the $\pi/2$ and the π pulse, then $\rho(\tau)$ is

$$\rho(\tau) = e^{-(i/\hbar)(H_z + H_{d0})\tau/2} X(\pi) e^{-(i/\hbar)(H_z + H_{d0})\tau/2} \times X\left(\frac{\pi}{2}\right)\rho(0)\{\text{c.c.}\}, \tag{A4}$$

where {c.c} stands for complex conjugate of the operators on the left of $\rho(0)$ and $X(\alpha)$ is an rf pulse applied along the X axis. Inserting $X^*(\pi)\,X(\pi)$ to the left of $X(\pi/2)$, we find in $\rho(\tau)$ the expresssion

$$X(\pi) e^{-(i/\hbar)(H_z + H_{d0})\tau/2} X^*(\pi) \tag{A5}$$

which is equal to

$$e^{-(i/\hbar)(-H_z + H_{d0})\tau/2}. \tag{A6}$$

Hence at τ the field inhomogeneities are refocused. We only need to calculate

$$\begin{aligned} \rho(\tau) &= e^{-(i/\hbar)H_{d0}(\tau)} x(\pi) X\left(\frac{\pi}{2}\right)\rho(0)\{\text{c.c}\}. \\ &= e^{-i\tau\Sigma_{i,j} a_{ij} I_{iz} I_{jz}}\left(-\sum_n I_{ny}\right) e^{i\tau\sum_{i,k} a_{ik} I_{iz} I_{kz}} \\ &= -\sum_n e^{-i\tau\Sigma_{i,j} a_{ij} I_{iz} I_{jz}} I_{ny} e^{i\tau\Sigma_{i,k} a_{ik} I_{iz} I_{kz}}. \end{aligned} \tag{A7}$$

Only the terms of the double sums where one of the operators is I_{nz} contribute to the evolution, so the expression reduces to

$$\sum_n e^{-i\tau I_{nz}\Sigma_{j\neq n} a_{nj} I_{jz}} I_{ny} e^{i\tau I_{nz}\Sigma_{k\neq n} I_{kz} a_{nk}} \tag{A8}$$

which, since $[I_{jz}, I_{nz}] = 0$ if $j \neq n$, can be written as

$$\sum_n \prod_{j\neq n} e^{-ia_{nj}\tau I_{nz} I_{jz}} I_{ny} \prod_{k\neq n} e^{ia_{nk}\tau I_{nz} I_{kz}}. \tag{A9}$$

The products can be arranged in the following order:

$$\cdots e^{-ia_{n2}\tau I_{nz} I_{2z}}\, e^{-ia_{n1}\tau I_{nz} I_{1z}} I_{ny}\, e^{ia_{n1}\tau I_{nz} I_{1z}}\, e^{ia_{n2}\tau I_{nz} I_{2z}} \cdots \tag{A10}$$

Consider the innermost product. We have (Ref. 22, Eq. 24)

$$\begin{aligned} &e^{-ia_{ni}\tau I_{nz} I_{iz}} I_{ny} e^{ia_{ni}\tau I_{nz} I_{iz}} \\ &\quad = I_{ny}\cos(a_{ni}\tau/2) - 2I_{nx} I_{iz}\sin(a_{ni}\tau/2). \end{aligned} \tag{A11}$$

Eventually, we are interested in $\langle I_y\rangle = \mathrm{Tr}(\rho I_y)$. The terms such as $I_{nx} I_{iz}$ will yield zero trace. Therefore we can write

$$\begin{aligned} \rho(\tau) &= e^{-(i/\hbar)H_{d0}\tau}\rho(0+)e^{(i/\hbar)H_{d0}\tau} \\ &= -\sum_n \prod_{j\neq n} \cos(a_{nj}\tau/2) \\ &\quad + \text{terms which do not contribute to } \langle I_y\rangle. \end{aligned} \tag{A12}$$

The echo height is

$$\begin{aligned} \langle I_y\rangle &= \mathrm{Tr}\{\rho I_y\} \\ &= -\mathrm{Tr}\left\{\left(\sum_k I_{ky}\right)\left(\sum_k \prod_{j\neq n} I_{ny}\cos(a_{nj}\tau)\right)\right\} \\ &= \mathrm{Tr}\left\{\sum_{j\neq k}\prod_{j\neq k} I_{ky}^2\cos(a_{kj}\tau)\right\} \\ &= -\sum_k \mathrm{Tr}\{I_{ky}^2\}\prod_{j\neq k}\cos(a_{kj}\tau) \\ &= \frac{1}{4}\sum_\kappa \prod_{j\neq k}\cos(a_{kj}\tau). \end{aligned} \tag{A13}$$

Note that this derivation applies readily to the calculation of the echo height in a spin echo double resonance experiment. In a SEDOR experiment, a spin S is observed by spin echo. At the time of the π pulse for the spin S, a π pulse is applied to neighboring spins $I_1, I_2, \ldots, I_N$.

[1] P.-K. Wang, C. P. Slichter, and J. H. Sinfelt, Phys. Rev. Lett. **53**, 82 (1984).
[2] H. E. Rhodes, P.-K. Wang, H. T. Stokes, C. P. Slichter, and J. H. Sinfelt, Phys. Rev. B **26**, 3559 (1982).
[3] P.-K. Wang, J.-Ph. Ansermet, C. P. Slichter, and J. H. Sinfelt, Phys. Rev. Lett. **55**, 2733 (1985).
[4] C. D. Makowka, C. P. Slichter, and J. H. Sinfelt, Phys. Rev. B **31**, 5663 (1985).
[5] E. L. Hahn and D. E. Maxwell, Phys. Rev. **88**, 1070 (1952).
[6] H. S. Gutowsky, D. W. McCall, and C. P. Slichter, J. Chem. Phys. **21**, 279 (1953).
[7] C. P. Slichter, *Principles of Magnetic Resonance*, 2nd ed. (Springer, Berlin, 1980).
[8] H. E. Rhodes, P.-K. Wang, C. D. Makowka, S. L. Rudaz, H. T. Stokes, C. P. Slichter, and J. H. Sinfelt, Phys. Rev. B **26**, 3569 (1982).
[9] J.-Ph. Ansermet, Ph.D. thesis, University of Illinois, 1985.
[10] D. M. Washecheck, E. J. Wucherer, L. F. Dahl, A. Ceriotti, G. Longoni, M. Manassero, M. Sansoni, and P. Chini, J. Am. Chem. Soc. **101**, 6110 (1979).

[11]R. F. Marzke, W. S. Glausinger, and M. Bayard, Solid State Commun. **18**, 1025 (1976).
[12]J. B. Boyce, Ph.D. thesis, University of Illinois, 1972.
[13]R. van Hardeveld, and F. Hartog, Surf. Sci. **15**, 189 (1969).
[14]M. J. Yacaman and J. M. Dominguez E., J. Catal. **64**, 213 (1980).
[15]T. Wang, C. Lee, and L. D. Schmidt, Surf. Sci. **163**, 181 (1985).
[16]M. A. van Hove, R. J. Koestner, P. C. Stair, J. P. Biberian, L. L. Kesmodel, I. Bartos, and G. A. Somorjai, Surf. Sci. **103**, 189 (1981).
[17]H. Hopster and H. Ibach, Surf. Sci. **77**, 109 (1978).
[18]L.-C. de Menorval and J. Fraissard, J. Chem. Soc. Faraday Trans 1 **81**, 2855 (1985).
[19]K. Foger and J. R. Anderson, Appl. Surf. Sci. **2**, 335 (1979); R. W. McCabe and L. D. Schmidt, Surf. Sci. **66**, 101 (1977).
[20]A. Crossley and D. A. King, Surf. Sci. **95**, 131 (1980); P. A. Thiel, R. J. Behm, P. R. Norton, and G. Ertl, Surf. Sci. **121**, L533 (1982); R. J. Behm, P. A. Thiel, P. R. Norton, and G. Ertl, J. Chem. Phys. **78**, 7437 (1983).
[21]P. R. Norton, J. A. Davies, D. C. Greber, C. W. Sitter, and T. E. Jackmann, Surf. Sci. **108**, 205 (1981).
[22]P.-K. Wang and C. P. Slichter, Bull. Magn. Reson. **8**, 3 (1986).
[23]O. N. Sorensen, G. W. Eich, M. H. Levitt, G. Bodenhausen, and R. R. Ernst, Progr. NMR Spectrosc. **16**, 163 (1983).
[24]F. J. M. Van de Ven and C. W. Hilbers, J. Magn. Reson. **54**, 512 (1983).